

# Poly(*N*-Vinyl Pyrrolidone-*b*-Dimethylsiloxane) Electrospun Nanofibers: Preparation, Characterization and Biological Response\*

Ivan L. Keranov<sup>1</sup>, Marc Michel<sup>1</sup>, Anelia Kostadinova<sup>3</sup>, Valerie Toniazio<sup>1</sup>,  
David Ruch<sup>1</sup>, Todorka Vladkova<sup>2</sup>

<sup>1</sup>Département of Advanced Materials and Structures, Centre de Recherche Public Henri Tudor,  
Esch sur Alzette, Luxembourg

<sup>2</sup>Department of Polymer Engineering, University of Chemical Technology and Metallurgy, Sofia, Bulgaria

<sup>3</sup>Institute of Biophysics and Biomedical Engineering, Bulgarian Academy of Science, Sofia, Bulgaria  
Email: aneliakk@yahoo.com

Received March 6, 2013; revised April 7, 2013; accepted April 14, 2013

Copyright © 2013 Ivan L. Keranov *et al.* This is an open access article distributed under the Creative Commons Attribution License, which permits unrestricted use, distribution, and reproduction in any medium, provided the original work is properly cited.

## ABSTRACT

Here we report electrospinning of Poly(dimethylsiloxane-*b*-vinyl pyrrolidone) (PDMS-*b*-PVP) based fibrous scaffold materials. The morphology, thermal properties, surface composition, hydrophilicity and fibers formation with different PDMS and PVP chain lengths were determined by using scanning electron microscopy (SEM), differential scanning calorimetry (DSC), X-ray photoelectron microscopy (XPS) and X-ray diffraction (RXD) water vapor uptake and water contact angle (WCA). The electrospinning parameters were controlled as well as fiber deposition area. The influence of polymer solution concentration on the morphology of electrospun fibers was also investigated. We checked out the applicability of the electrospun fibers for tissue engineering by the investigation of their capability to support fibroblast cell adhesion, cell growth and proliferation.

**Keywords:** Electrospinning; Nanofibers; Amphiphilic Block Copolymers; PDMS; PVP; SEM

## 1. Introduction

Electrospinning is a unique technique that can produce non-woven fibrous materials with fiber diameters ranging from nanometers scale to micrometers scale. The important advantages of this technique are the production of very thin fibers with large surface areas, excellent mechanical properties, facile modification and ease of process [1].

Block copolymer scaffolds can be electrospun in fibers, combining the unique physicochemical and biological properties and the ability to control the fibers structure during electrospinning process by the control of different parameters [2], which offers opportunity for new biomaterials fabrication with unusual properties. The polymer material selection plays a key role in the fabrication of scaffold with desired properties. They can be achieved by combination of homo polymers advantages in blended solutions (natural and/or synthetic polymers), copoly-

merization techniques, hybrid materials, processing techniques [1-4] and surface modification techniques of the fibers [5] with possible variety of biomedical application.

By block copolymer, electrospinning can be possible to fabricate super hydrophobic microphase-separated fibers [6] or ultrafine fibers made from amphiphilic PEG-*b*-PDMS-*b*-PEG copolymer [7] or moreover the electrospinning of block copolymers increases the hydrophilicity, compared with their casted film forms [8]. Furthermore, electrospinning of different types of synthesized block copolymers gives more possibilities for new scaffolds fabrication. Therefore, the electrospinning of block copolymers is not only promising for applications involving surface chemistry, drug delivery, tissue engineering and multifunctional textiles, but also is of scientific interest.

Our researches revise in the scientific literature showed, there are no reports on preparation of amphiphilic Poly(dimethylsiloxane-*b*-vinyl pyrrolidone) (PDMS-*b*-PVP) based fibrous scaffold materials. PDMS-based

\*This research was supported financially by the Fond National de Recherche, Luxembourg.

amphiphilic copolymers containing PVP, PEG or other biocompatible, hydrophilic and water soluble block are attractive for the preparation of materials with specific and unique properties and possible biomedical application. Recently, we have synthesized and characterized in detail amphiphilic PDMS-*b*-PVP copolymers by free radical polymerization by means with non-commonly used PDMS macroazoinitiators [9]. The present study demonstrates the possibility of fabrication of novel poly(dimethylsiloxane-*b*-vinyl pyrrolidone) fibrous materials by screen controlled electrospinning. The fiber morphology was studied by scanning electron microscopy (SEM) and the thermal properties were studied by DSC. The crystalline structure of the novel materials was investigated by X-ray diffraction (XRD). The surface chemical composition of the electrospun fibers was determined by X-ray photoelectron spectroscopy (XPS). Swelling properties were also determined in order to evaluate hydrophilicity of the electrospun copolymer fiber mats. The biological response of the electrospun fiber mats was evaluated with human fibroblast cells.

## 2. Experimental Section

### 2.1. Materials

All the solvents as chloroform, THF, methanol, ethanol, and diethyl ether were purchased from Carl Roth and used without purification. Poly(dimethylsiloxane-*b*-vinyl pyrrolidone): PDMS<sub>4.6K</sub>-*b*-PVP<sub>177.5K</sub>, PDMS<sub>4.6K</sub>-*b*-PVP<sub>56.8K</sub>, PDMS<sub>4.6K</sub>-*b*-PVP<sub>0.45K</sub>, PDMS<sub>10K</sub>-*b*-PVP<sub>21.4K</sub>, PDMS<sub>10K</sub>-*b*-PVP<sub>13.9K</sub> and PDMS<sub>10K</sub>-*b*-PVP<sub>5.1K</sub> were purified by dissolving in tetrahydrofuran and precipitated in diethyl ether 3 times then dried at 40 °C for 48 hours.

### 2.2. Synthesis of PDMS-*b*-PVP

The amphiphilic block copolymer with two different PDMS chain lengths was synthesized and characterized in detail in our previous work [9]. Briefly, the block copolymer synthesis, containing dimethylsiloxane and 1-vinyl-2-pyrrolidone was achieved with conventional radical polymerization (CRP). PDMS macroazoinitiator (MAI) was used as initiator for the polymerization of 1-vinyl-2-pyrrolidone. The preparation of the copolymers was carried out in 10 ml schlenk flasks, each one containing 5 ml dichloromethane and different molar ratio of MAI and 1-vinyl-2-pyrrolidone. The mixtures were bubbled with Ar stream, sealed and after that all tubes were immersed into thermostatically controlled oil bath at 70 °C for 12 h. The resulting block copolymers were dissolved in chloroform, slowly precipitated in diethyl ether, filtered and the obtained white products were dried in vacuum at 40 °C for 48 h.

### 2.3. Electrospinning Set Up

The electrospinning setup we used in this study is presented in **Figure 1**. PDMS<sub>4k</sub>-*b*-PVP and PDMS<sub>10k</sub>-*b*-PVP with different molecular weights were dissolved in chloroform at various concentrations (10 - 23 wt%), stirred at room temperature for 12 hours.

Polymer solution was placed into 5 ml syringe mounted in a syringe pump (model KDS 200, KD Scientific Inc). The syringe was capped with (1.0 × 55 mm) blunt end needle. The positive lead from high voltage supply (CZE-30PN0.25, Matsusada Precision Inc., Japan) was attached via an alligator clip to the external surface of the metal syringe needle. A round-shape (D = 5.0 cm) grounded collector fabricated from brass was used. The distance from collector and the tip of the syringe was fitted to 14 cm. At the onset of the electrospinning, the syringe pump was set to deliver source solution at rate 20 µl/min and simultaneously, the high voltage was applied across the source solution and grounded collector (+10 - 19 kV). Thin alumina screen (80 × 80 mm) with varied bend angles, attached to the metal needle was used to control fibers deposition on the grounded collector.

### 2.4. Cells

Human fibroblasts were prepared from fresh skin biopsy and used up to the ninth passage. The cells were grown in Dulbecco's minimal essential medium (DMEM) containing 10% fetal bovine serum (Sigma) in a humidified incubator with 5% CO<sub>2</sub>. For the experiments, the cells were harvested from nearly confluent cultures with 0.05% try p sin/0.6 mM EDTA (Sigma).

### 2.5. Cell Growth

The cell proliferation was determined via modified lactate dehydrogenase (LDH) assay (Hoffman La Roche,

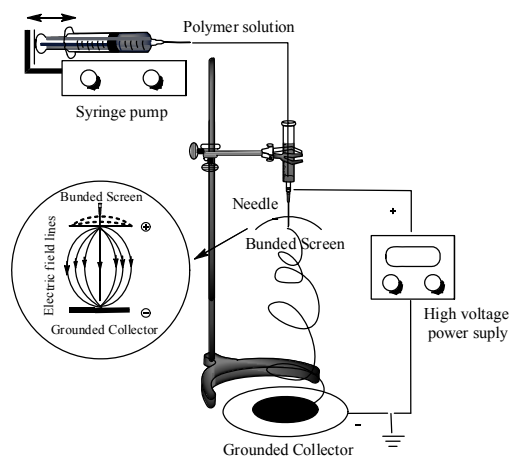


**Figure 1.** Schematic illustration of our electrospinning system.

Penzberg, Germany) after 1, 3, and 5 days of incubation. Briefly, at the indicated incubation time, the medium was removed and the cells were lysed with 0.5 mL 1% Triton-X 100 in PBS under shaking for 1 h. The cells lysates were centrifuged at  $2000 \times g$  for 5 min. Thereafter, 100  $\mu$ L of LDH test solution was added to each well, and the samples were incubated for 15 min at room temperature in dark. The reaction was stopped with 50  $\mu$ L 1 M HCl. The absorbance was measured with Spectra Flour Plus plate reader (Tecan, Crailsheim, Germany) at 492 nm. The reference wavelength was at 620 nm. Each experiment was quadruplicated.

## 2.6. Actin Staining

Overall cell morphology was observed by actin staining. Fibroblasts with density of  $1.5 \times 10^5$  cells/ml were cultivated on cover glasses ( $18 \times 18$  mm), placed in 6-well plates for 24 h. After the incubation period, the non-adhered cells were removed by triple rinsing with PBS (pH 7.4). The adhered cells were fixed with 1 mL 3% solution of paraformaldehyde (PFA) for 15 minutes at room temperature. The fixed cells were permeabilized using 1 mL 0.5% solution of Triton X-100 for 5 minutes and then incubated with 1 mL 1% solution of serum bovine albumin (BSA) for 15 minutes. The samples were washed three times with PBS (pH 7.4) and incubated for 30 min at room temperature with BODIPY 558/568 phalloidin. Again, the samples were washed three times with PBS and once with distilled water, and then were installed on objective glasses by Mowiol. The samples were analyzed using inverted fluorescent microscope (Leica DMI3000 B, Leica Microsystems GmbH, Germany) with objective HCX PL FLUOTAR 63x/1.25 oil.

## 3. Characterization

### 3.1. Differential Scanning Calorimetry (DSC) Measurement

DSC measurements were performed with a Netzsch DSC 204 F1 Phoenix apparatus. The sample of mass weight about 3 mg placed in aluminum pan with pierced lid was heated in temperature range from  $-150^\circ\text{C}$  to  $200^\circ\text{C}$  at heating rate 10 K/min. The system was purged continuously with nitrogen with flow rate at 100 ml/min.

### 3.2. XPS Analysis

XPS spectra of C 1s, O 1s, N 1s and Si 2p of the surface are recorded using XPS (Hemispherical Energy Analyzer SPECS, PHOIBOS 150) employing a monochromatic Al  $K\alpha$  X-rays operating at 200 W with an anode voltage of 12 kV. The pressure in the analysis chamber was  $10^{-9}$  mbar. The XPS spectra were referenced with respect to the C 1s peak at 284.6 eV originating from carbon con-

tamination. Core peaks were analyzed using a nonlinear Shirley-type background and fitted using 70% Gaussian, 30% Lorentzian line shapes.

### 3.3. Contact Angle Measurement

The contact angles of water were measured on the chloroform solution cast films and electrospun films. The contact angles were measured on a OCA 15 goniometer, by image processing (CCD camera, resolution  $752 \times 582$ ) of sessile drop with SCA 20 software. At least 6 droplets of freshly distilled ultra pure water were averaged. Drops of purified water, 3  $\mu$ L, were deposited onto the film surface to form sessile drops using 1 ml micro-syringe equipped with needle ( $0.51 \times 50$  mm) and a static image was taken after Sections 2 and 3. Contact angles on different parts of the film were measured and averaged.

### 3.4. Water Vapor Uptake

In order to determinate changes in hydrophilicity of the electrospun fiber mats water vapour sorption was investigated. The water vapour uptake of the electrospun fibre mats was determined by measuring the change in the weight before and after the hydration in exicator with constant weight. The fibre mats (0.1 g from each sample) were putted in glass filters and kept 2 weeks in exicator with relative humidity (100%). After that, the wetted samples were determined as quickly as possible. The dried samples were determined after completely drying at  $40^\circ\text{C}$  for 48 h. The water vapour uptake was defined as following equation:

$$\text{Water vapor uptake} = (m_1 - m_0)/m_0 \times 100\%$$

Where,  $m_0$  and  $m_1$  are the masses of fibers after drying and after storage in exicator. The measurements were carried out at room temperature ( $22^\circ\text{C}$  -  $24^\circ\text{C}$ ).

### 3.5. SEM Observation

Scanning electron microscopy (SEM) Quanta FEG 200 (FEI Europe BV, Branch Belgium) equipped with energy dispersive X-ray (EDX) system for identifying the elemental composition of the specimen, or an area of interest was used. The morphology of the self-assembled block copolymer films was observed at electron acceleration of 7 kV without Au/Pd coating for the samples, and images at various levels of magnification were captured.

### 3.6. RXD Measurement

We performed wide-angle X-ray scattering (WAXS) experiments using the equipment Panalytical X'Pert Pro MPD configured with the transmission mode. The beam was generated at 40 kV and 45 mA by means of an X-ray tube equipped with a copper anode which enables to

analyze the material periodicities with the  $K\alpha$  copper radiation (wavelength  $\lambda = 1.54 \text{ \AA}$ ). As incident optics, we utilized a focusing mirror, and as secondary optics we utilized the PIXcel detector. These two optics were configured with specific slits which enable to get a high resolution and a low background in the angular range of interest ( $5^\circ$  to  $50^\circ$ ). A spinner was used as sample-holder with a revolution time of 4 s to put the maximum of dipoles in scattering position. The intensity ( $I$ )-2 theta ( $2\theta$ ) curves were treated with the software PeakFit to extract the background and perform the deconvolution of the scattering peaks. On the basis of Bragg relationship  $2d_i \sin\theta_i = n\lambda$  ( $n$  is the scattering order), we assessed structural periodicities  $d_i$  from the position of the peaks  $\theta_i$ .

## 4. Result and Discussion

Electrospun nanofibrous scaffolds possess an extremely high surface-to-volume ratio, tunable porosity and malleability to conform over a wide variety of sizes and shapes. For their biomedical application, its physical and biological properties, such as hydrophilicity, mechanical modulus and strength, biodegradability, biocompatibility, and specific cell interactions, are largely determined by the materials chemical composition. The use of block copolymers is a viable scheme to generate new materials of desirable properties. When properly implemented, the performance of electrospun scaffolds based on copolymers can be significantly improved when compared to that of homopolymers. For example, biodegradable hydrophobic polyesters generally have good mechanical properties, but lack cell affinity for tissue engineering. The incorporation of proper hydrophilic polymer segment can increase cell affinity. Besides the cell affinity, the mechanical properties, morphology, structure, pore size and distribution, biodegradability and other physical properties can also be tailored by using copolymers. Moreover, with amphiphilic copolymers as protecting molecules to encapsulate drug molecules, electrospun scaffolds can be used for drug release in controlled manner.

In the present study, diblock copolymers based on poly(dimethylsiloxane) and poly(*N*-vinyl pyrrolidone) blocks (PDMS-*b*-PVP) with different chain lengths were used. They were synthesized by conventional radical polymerization, using PDMS macroazoinitiator and characterized in detail [9].

### 4.1. Effect of the Screen on Fibers Deposition

During the spinning process we controlled the fibers deposition area onto collector by alumina screen attached to the metal needle (**Figure 1**) with bend angles of  $0^\circ$ ,  $30^\circ$  and  $60^\circ$ . The effect we obtained was total concentration of electrospun fibers onto collector surface with

round shape. No fibers were spreaded out of the collector area. The effect of fiber concentration was more expressive when the bend angle was  $30^\circ$ , which resulted in decreasing of fibers area deposition. The strongest effect was achieved at bend angle  $60^\circ$  the deposited fibers were concentrated onto very small area. We explain this fact with that the screen plays role as a “lens”, concentrating the electric field between positive charged electrode and negative charged collector area (**Figure 1**, in the circle). Further increasing of angle does not change more the fibers deposition area. The effect on fibers morphology will be discussed elsewhere.

### 4.2. The Effect of Polymer Solution Concentration

We attempted electrospinning of PDMS-*b*-PVP's with different composition dissolved in chloroform at various solution concentrations. In **Table 1** are summarized electrospinning conditions and fiber morphology of electrospun fiber scaffolds.

Detailed morphological information was obtained by scanning electron microscopy (SEM). **Figure 2** shows SEM images representing different morphologies obtained from PDMS-*b*-PVP block copolymers solutions with different concentration (10 - 23 wt%), fixed tip-to-collector distance (14 cm), flow rate (20  $\mu\text{L}/\text{min}$ ) and varied electric field (6 - 19 kV). **Figures 2(A)-(C)** show electrospun copolymers with concentration between 10 - 12 wt% and applied voltage from 6 to 19 kV. We observed that in this concentration range and applied high voltage the layer deposited onto the collector is made only from spherical particles (**Figure 5(A)**), because the viscoelastic forces of the solution is not enough to withstand the elastic forces. The process is more like electrospray. At high magnification it can be seen that the particles are quite polydispers and with diameter ranging from 150 nm to 1.4  $\mu\text{m}$ . The voltage does not change the polydispersity.

With the increase of block copolymer solution concentration (15 wt%) fibers appears, but with beads (**Figures 2(D)-(F)**) and the shape of the beads is elongated and indentations are observed, indicating for hollow beads (**Figures 2(E)** and **(F)**). The diameter of elongated beads is between 2.1  $\mu\text{m}$  and 3  $\mu\text{m}$  and the length 7 - 11  $\mu\text{m}$ . When the concentration of the copolymer solution increase to 17 wt% for high molecular weight copolymer or 22 wt% for low molecular weight copolymer, the morphology of the electrospun copolymers is changed from fibers with elongated beads to smooth and uniform fibers (**Figures 2(G)-(I)**). The diameters of fibers are summarized in **Table 1**. At 17 wt% the diameter range between 2.6  $\mu\text{m}$  and 3.4  $\mu\text{m}$ , but small present of fibers under 1  $\mu\text{m}$  can be seen. It must be note that the molecular weight of the copolymers was also an important factor



Table 1. Characteristic properties of the copolymers, electrospinning conditions and fibers morphology.

Block copolymer	Total M <sub>w</sub> , (kDa)	PD	Concentration, (wt%)	Voltage, (kV)	Distance, (cm)	Flow rate, (μL/min)	Morphology	Fiber diameter
PDMS <sub>4.6K</sub> - <i>b</i> -PVP <sub>177.5K</sub>	182.1	1.17	10	6 - 19	14	20	Beads	2.6 μm -3.4 μm
PDMS <sub>4.6K</sub> - <i>b</i> -PVP <sub>177.5K</sub>	182.1	1.17	15	6 - 19	14	20	Fibers with beads	
PDMS <sub>4.6K</sub> - <i>b</i> -PVP <sub>177.5K</sub>	182.1	1.17	17	16	14	20	Uniform fibers	
PDMS <sub>4.6K</sub> - <i>b</i> -PVP <sub>56.8K</sub>	61.4	1.61	10	6 - 19	14	20	Beads	912 nm - 2.72 μm
PDMS <sub>4.6K</sub> - <i>b</i> -PVP <sub>56.8K</sub>	61.4	1.61	15	6 - 19	14	20	Fibers with beads	
PDMS <sub>4.6K</sub> - <i>b</i> -PVP <sub>56.8K</sub>	61.4	1.61	19	14 - 19	14	20	Uniform fibers	
PDMS <sub>4.6K</sub> - <i>b</i> -PVP <sub>0.45K</sub>	5.1	1.23	12	6 - 19	14	20	Beads	650 nm - 980 nm
PDMS <sub>4.6K</sub> - <i>b</i> -PVP <sub>0.45K</sub>	5.1	1.23	17	6 - 19	14	20	Fibers with beads	
PDMS <sub>4.6K</sub> - <i>b</i> -PVP <sub>0.45K</sub>	5.1	1.23	23	14 - 19	14	20	Uniform fibers	
PDMS <sub>10K</sub> - <i>b</i> -PVP <sub>21.4K</sub>	31.4	1.98	10	6 - 19	14	20	Beads	530 nm - 2.04 μm
PDMS <sub>10K</sub> - <i>b</i> -PVP <sub>21.4K</sub>	31.4	1.98	15	6 - 19	14	20	Fibers with beads	
PDMS <sub>10K</sub> - <i>b</i> -PVP <sub>21.4K</sub>	31.4	1.98	18	14 - 19	14	20	Uniform fibers	
PDMS <sub>10K</sub> - <i>b</i> -PVP <sub>13.9K</sub>	23.9	1.81	12	6 - 19	14	20	Beads	870 nm - 2.01 μm
PDMS <sub>10K</sub> - <i>b</i> -PVP <sub>13.9K</sub>	23.9	1.81	16	6 - 19	14	20	Fibers with beads	
PDMS <sub>10K</sub> - <i>b</i> -PVP <sub>13.9K</sub>	23.9	1.81	22	14 - 19	14	20	Uniform fibers	
PDMS <sub>10K</sub> - <i>b</i> -PVP <sub>5.1K</sub>	15.1	1.05	12	6 - 19	14	20	Beads	1.2 μm - 2.46 μm
PDMS <sub>10K</sub> - <i>b</i> -PVP <sub>5.1K</sub>	15.1	1.05	15	6 - 19	14	20	Fibers with beads	
PDMS <sub>10K</sub> - <i>b</i> -PVP <sub>5.1K</sub>	15.1	1.05	22	14 - 19	14	20	Uniform fibers	

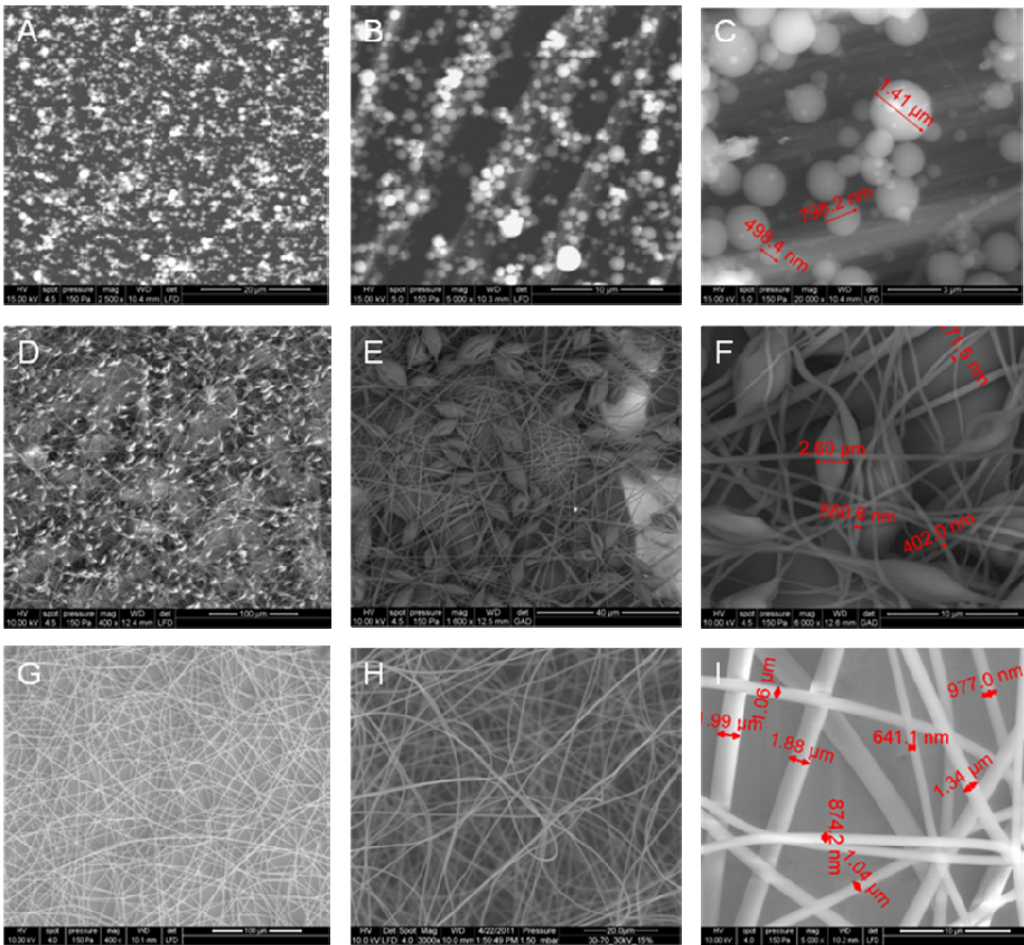


Figure 2. SEM images at different magnification (A), (B) and (C), from 3 μm to 20 μm for spherical particles and (D)-(I), from 10 μm to 100 μm for fibers) of PDMS-*b*-PVP electrospun fibers from chloroform solutions with different concentrations 10 wt% (A), (B) and (C), 15 wt% (D), (E) and (F) and 18 wt% (G), (H) and (I).

for spinning. With the low molecular weight copolymer and wide range of concentrations the jet broke up into droplets and produced only spherical particles (See **Table 1**). Increasing the molecular weight lower copolymer solution concentration is needed to produce uniform fibers and the chains can entangle sufficiently to provide stability to the spinning jet.

### 4.3. Thermal Properties

The fibers mats thermal properties were characterized with differential scanning calorimetry (DSC) and thermogravimetry analysis (TGA). The shape of DSC thermogram on **Figure 3** is very similar to the thermograms of block copolymers PDMS-*b*-PVP that we already previously reported [9]. As can be seen one characteristic transition for PDMS phase  $T_g$  PDMS and two transitions of PVP phase,  $T_g$  PVP and  $T_m$  PVP (**Figure 3**) were observed. From the literature data it is well known that PDMS has the extremely low  $T_g$  of  $-127^\circ\text{C}$ .

In this study we detected that the  $T_g$  of PDMS segment ( $-127^\circ\text{C}$  according to the literature) in the PDMS-*b*-PVP fiber mats decreases to  $-110^\circ\text{C}$  and melting endotherm for PDMS was not observed. Probably this is due to the presence of PVP segment and lack of free crystallizable amorphous regions, because of not so fast solvent evaporation during the electrospinning process.  $T_g$  of PVP segment in all electrospun block copolymers decreases and  $T_m$  increases in compare with homo-PVP values [9], due to the presence of PDMS segment and apparently were affecting as plasticizer, also observed elsewhere [11]. Finally, a comparison of Thermogravimetry analysis (TGA) (**Figure 4**) of the electrospun fiber mats, it was detected significant presence of water after 24 hours storage at room temperature (**Figure 4**, TG curve 1 and DTG curve 1\* (small figure)).

This decreases slightly the  $T_g$  values of PVP when the water is presented in the fibers mat and conversely slightly increased after drying at  $40^\circ\text{C}$  for 48 hours. This could be explained with the strong hydrophilic character of PVP segment in the fibers mat, attracting water molecules which rearranges the polymer chains arrangement and thus changes the  $T_g$  values. There are two steps of degradation between  $180^\circ\text{C}$  -  $250^\circ\text{C}$  for PVP block and about  $460^\circ\text{C}$  -  $600^\circ\text{C}$  for PDMS block from fibers mats.

**Water vapor uptake** studies were performed on the electrospun fibers with different PVP content in order to evaluate hydrophilicity and the changes in morphology at room temperature and constant humidity. Well dried fiber mats (48 hours at  $40^\circ\text{C}$ ) were placed onto ceramic surface in exicator filled with deionized water and without contact with water then the absorption was measured in the first 24 hours and then for two weeks. Absorption data are presented in **Figure 5**. It is obvious that for both

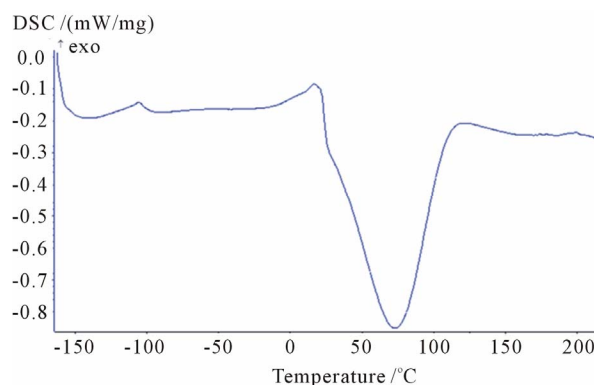


**Figure 3.** DSC thermograph of PDMS<sub>4.6K</sub>-*b*-PVP<sub>177.5K</sub> electrospun fibers mat from 20 wt% chloroform solution. We observed characteristic transition for PDMS phase and two transitions of PVP phase, respectively:  $T_m$  of PDMS ( $-110^\circ\text{C}$ ) and  $T_g$ , ( $22^\circ\text{C}$ ),  $T_m$  ( $65.9^\circ\text{C}$ ) of PVP.

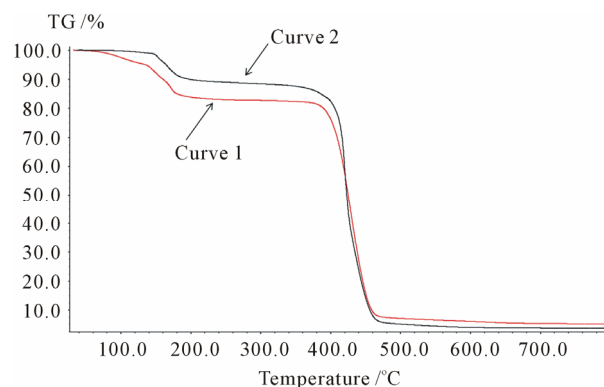


**Figure 4.** TGA thermogram of PDMS<sub>4.6K</sub>-*b*-PVP<sub>177.5K</sub> electrospun fibers, after 24 hours storage at room temperature (Curve 1, (presence of water molecules)) and after 48 hours drying in vacuum oven at  $40^\circ\text{C}$  (Curve 2 (lack of water)).

fibers containing PDMS<sub>4.6K</sub> and PDMS<sub>10K</sub> water absorption strongly increase in the first 8 hours (**Figures 5(A)** and **(B)**).

The electrospun fibers from (PDMS<sub>4.6K</sub>-*b*-PVP<sub>0.45K</sub>) with low PVP content absorbed small amount of water, whereas the fibers with low PVP content, but longer PDMS chain (PDMS<sub>10K</sub>-*b*-PVP<sub>5.1K</sub>) absorbed relatively higher amount of water. With increasing of PVP content the hydrophilicity increases and for samples with the highest PVP content (PDMS<sub>10K</sub>-*b*-PVP<sub>21.4K</sub> and PDMS<sub>4.6K</sub>-*b*-PVP<sub>177.5K</sub>) appeared very hydrophilic. It is of interest to note that the water absorption equilibrium was reached after approximately 8 days for both copolymer fiber mats. The surface hydrophilicity of the fiber mats were also examined by water contact angle (WCA) measurement (**Figure 5(C)**). The surface of block copolymer fibers is highly hydrophilic in the case of fibers electrospun from copolymer with short PDMS chain, reporting contact angles between  $36^\circ$  for PDMS<sub>4.6K</sub>-*b*-PVP<sub>0.45K</sub> and  $24^\circ$  for PDMS<sub>4.6K</sub>-*b*-PVP<sub>177.5K</sub> (**Figure 5(C)**). Water spread out

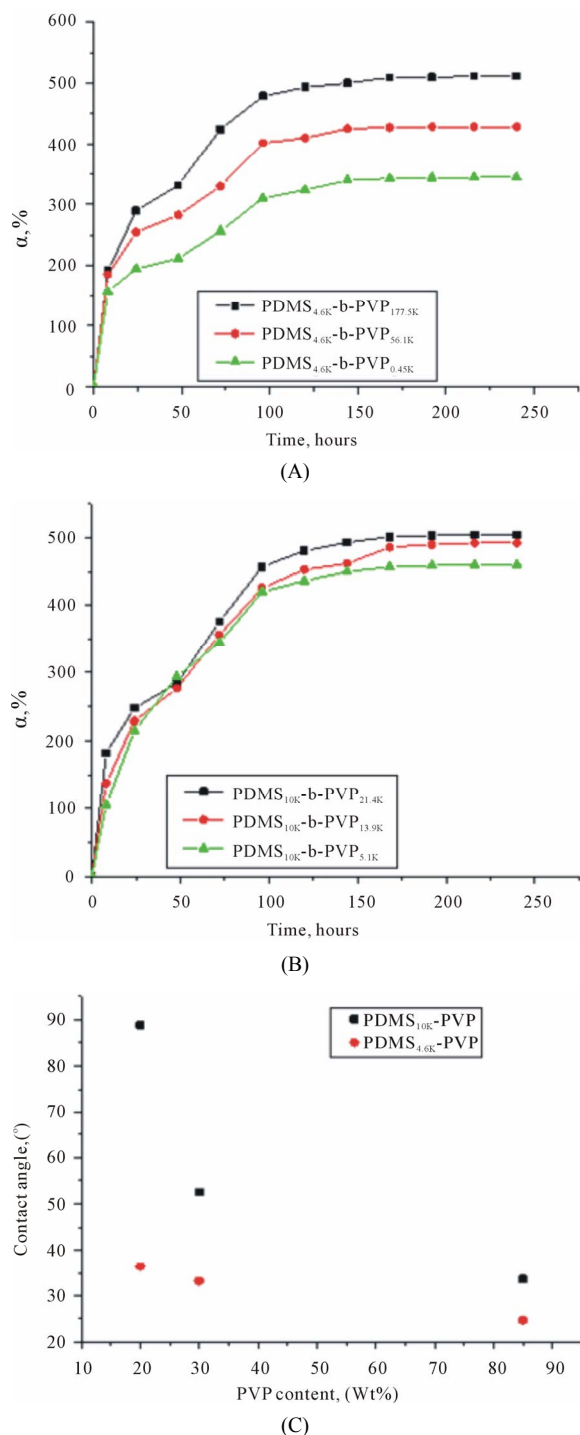


**Figure 5.** Equilibrium water absorption for: (A) PDMS<sub>4.6K</sub>-b-PVP<sub>177.5K</sub>, PDMS<sub>4.6K</sub>-b-PVP<sub>56.8K</sub> and PDMS<sub>4.6K</sub>-b-PVP<sub>0.45K</sub> copolymer fibers; (B) PDMS<sub>10K</sub>-b-PVP<sub>21.4K</sub>, PDMS<sub>10K</sub>-b-PVP<sub>13.9K</sub> and PDMS<sub>10K</sub>-b-PVP<sub>5.1K</sub> copolymer fibers; (C) Water contact angle of copolymer fiber mats.

immediately upon contact with the surface of fiber mats. On the other hand, the fiber mats with longer PDMS chain gave contact angle of 88° for PDMS<sub>10K</sub>-b-PVP<sub>5.1K</sub> and 52° for PDMS<sub>10K</sub>-b-PVP<sub>13.9K</sub> and were more hydro-

phobic except PDMS<sub>10K</sub>-b-PVP<sub>21.4K</sub> than the copolymer fibers with short PDMS chain (**Figure 5(C)**). It must be note also that the fibers morphology changes completely after reaching the swelling equilibrium from fibers to polymer gel (**Figure 6**).

This is because PVP is water-soluble polymer and PDMS do not prevent the inhomogeneous fiber mats from complete dissolving/swelling, resulting at the end in lack of fibrous structure. The electrospinning of PDMS-b-PVP generates a highly hydrophilic fiber mat and this could be advantageous in tissue engineering or may have potential application in drug release systems.

#### 4.4. XPS Characterization

Both the wide energy survey scans and C1s, O1s, N1s and Si2p core-level spectra were recorded from electrospun PDMS-b-PVP copolymer fibers collected on Al foils (**Figure 7**).

Results of XPS analysis are shown in **Figure 7** and **Table 2**.

The surfaces of the fiber mats are seen to consist of carbon, oxygen and silicon from PDMS and carbon, oxygen and nitrogen coming from PVP. The C 1s core-level spectrum of the PDMS-b-PVP fibers shown on **Figure 7** can be deconvoluted by curve fitting into three components: the sp<sup>3</sup>-hybridized carbon peak with a binding energy (BE) at 284.6 eV corresponding to the two side CH<sub>3</sub>- groups in PDMS block, -CH- unit and the -CH<sub>2</sub>- unit at 285.0 eV in the PVP backbone and CH<sub>2</sub> near to C=O in the PVP ring (**Figure 7**, labeled C-H and C-H<sub>2</sub>), the peak with BE 285.6 eV for -CH<sub>2</sub> adjusted to the nitrogen atom in PVP ring (**Figure 7**, C-N labeled) and the sp<sup>2</sup>-hybridized carbon peak with BE 287.5 eV corresponding to C=O unit from PVP ring. The O 1s core-level deconvoluted spectrum of the copolymer fiber mats shows two components at 531.5 eV corresponding to oxygen in PDMS backbone (**Figure 7**, O-Si labeled) and at 530.6 eV corresponding to oxygen from C=O unit from PVP ring. It is interesting to note that the atom percentage of the carbon and nitrogen decreases and the atom percentage of the silicon and oxygen increases

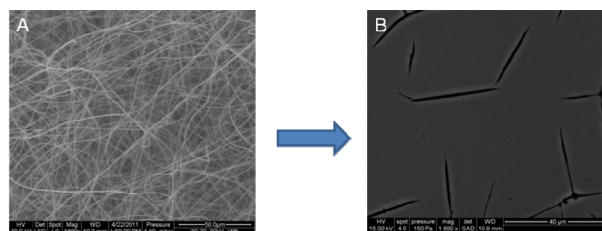


**Figure 6.** Effect of water absorption on the morphology of electrospun PDMS-b-PVP copolymer uniform fibers obtained at 16 kV, total polymer concentration 18 wt%. (A) before water absorption and (B) after 24 hours water absorption.

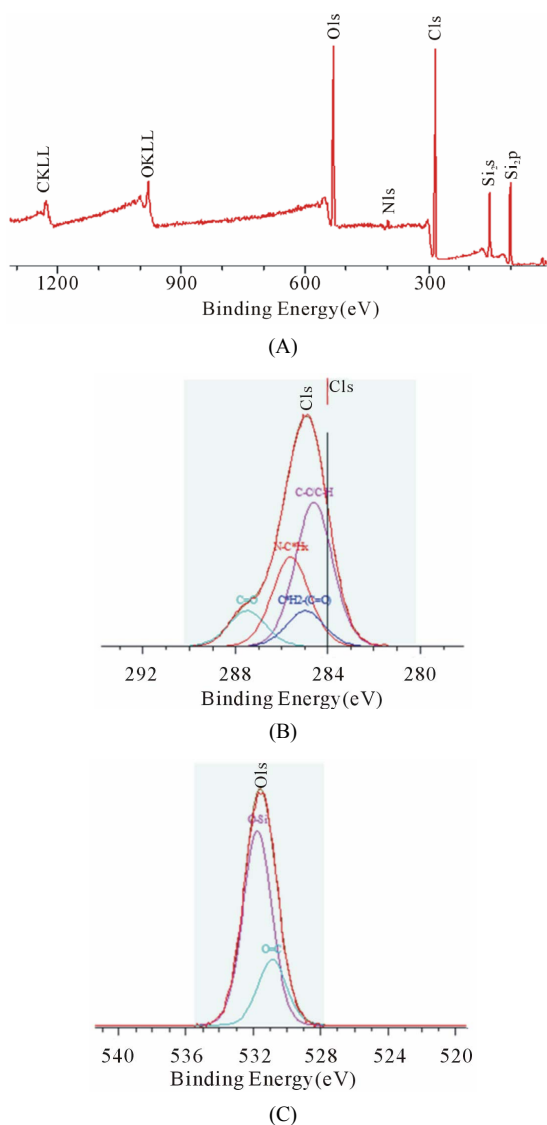


**Figure 7.** XPS wide scan spectrum (A), (B) 1s core-level spectrum and (C) O 1s core-level spectrum of PDMS<sub>10K</sub>-*b*-PVP<sub>21.4K</sub> fiber mat obtained at 16 kV and 18 wt% total polymer concentration.

simultaneously for both copolymer fiber mats (PDMS<sub>4.6K</sub> and PDMS<sub>10K</sub>). clearly evident from **Table 2**. The decrease of the total carbon amount and nitrogen amount in the surface layer of the electrospun fibers and, is due to the decrease of molecular weight of PVP block (compare with **Table 1**) in the copolymer and this leads to the increase of silicon and oxygen, coming from PDMS block, which fixed for all copolymers.

#### 4.5. XRD Analysis

XRD analyses were performed to determine the structure of the fibers. **Figure 8** illustrated the X-ray diffraction pattern for PDMS<sub>10K</sub>-*b*-PVP fiber mats. It were detected two peaks, one at 20.55° corresponding to PVP segment

and peaks between 11.2° and 13.9° related with PDMS segment. Crystalline peaks could not be detected at room temperature for all electrospun fiber mats.

**Figure 8** X-ray diffraction patterns of PDMS<sub>10K</sub>-*b*-PVP<sub>21.4K</sub>, PDMS<sub>10K</sub>-*b*-PVP<sub>13.9K</sub> and PDMS<sub>10K</sub>-*b*-PVP<sub>5.1K</sub> copolymer fibers mats.

#### 4.6. Human Fibroblast Cell onto PDMS-*b*-PVP Fibers

The next part of this work focuses on the applicability of PDMS-*b*-PVP fibers for tissue engineering proposes. For this reason we demonstrate that the fibers support cell adhesion and stimulate cell growth and proliferation.

#### 4.7. Overall Cell Morphology

The overall cell morphology by actin staining of fibroblasts adhering for 24 h on silicon wafer PDMS<sub>4.6K</sub>-*b*-PVP<sub>56.8K</sub>, PDMS<sub>4.6K</sub>-*b*-PVP<sub>0.45K</sub>, PDMS<sub>10K</sub>-*b*-PVP<sub>13.9K</sub> and copolymer fibers (**Figures 9(B)-(D)**) are represented in **Figure 9**.

It is evident that the fibroblast number on all three PDMS-*b*-PVP copolymer fibers is less, compared to that of the control silicon wafer (**Figures 9(B)-(D)**). In addition, the fibroblasts on the PDMS<sub>10K</sub>-*b*-PVP electrospun fiber surfaces represent a round shape and there is not have stress fiber actin is defuse (**Figure 9(D)**) because of their disturbed spreading. Cells on **Figure 9(B)** presented good stress fibers. This could be explained by the high hydrophilic nature of these fibers (**Figure 9(B)**) characterizing, with a WCA of about 36° (See **Figure 5**). For samples with WCA 88° (**Figure 9(D)**) which is hydrophobic compared with the first one were also observed fibroblast cell with round shape. It is well known [10] that the strong hydrophilic surfaces do not support the initial interaction with living cells. On the other hand, hydrophobic surfaces do not also support cell spreading and proliferation.

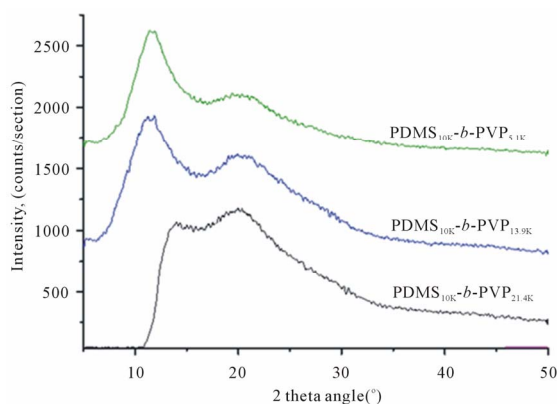
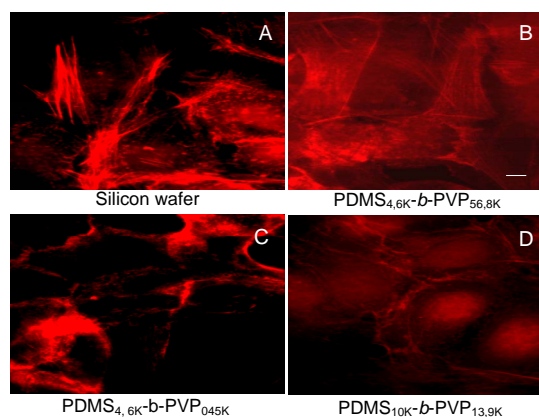
#### 4.8. Cell Growth

The capability of different electrospun PDMS-*b*-PVP fibers to support the cell growth over a period of 7 days was studied using LDH assay. As illustrated in **Figure 10** PDMS-*b*-PVP promoted an increase cell growth with each day of incubation. Cell proliferation however was reused witch increasing. LDH method clearly shows that the cells grow well on 1, 3 and 7 day on PDMS<sub>4.6K</sub>-*b*-PVP<sub>56.8K</sub> and PDMS<sub>4.6K</sub>-*b*-PVP<sub>0.45K</sub>, and less on PDMS<sub>10K</sub>-*b*-PVP<sub>13.9K</sub>. The significant statistically changes we found between the first and third days of cell proliferation and this we indicated it with 1 asterix. With two asterix we show statistically changes between PDMS<sub>10K</sub>-*b*-PVP<sub>13.9K</sub> and PDMS<sub>4.6K</sub>-*b*-PVP<sub>56.8K</sub>. The cell proliferation confirms our morphological investigation and once again showed



**Table 2.** Atomic composition as derived from XPS analysis of varied PDMS-*b*-PVP fiber mats.

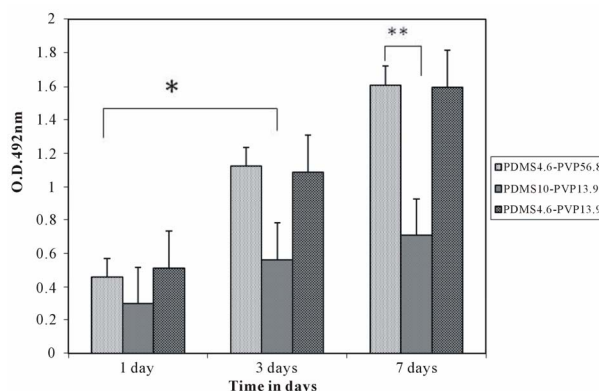
Sample	C 1s at. (%)	O 1s at. (%)	N 1s at. (%)	Si 2p at. (%)	C/Si	O/Si	C/N	O/N
PDMS <sub>4.6K</sub> - <i>b</i> -PVP <sub>177.5K</sub>	71.40	14.60	10.13	3.86	18.50	3.78	7.05	1.44
PDMS <sub>4.6K</sub> - <i>b</i> -PVP <sub>56.8K</sub>	68.04	17.59	7.71	6.66	10.22	2.64	8.82	2.28
PDMS <sub>4.6K</sub> - <i>b</i> -PVP <sub>0.45K</sub>	59.98	21.14	5.20	13.69	4.38	1.54	11.53	4.06
PDMS <sub>10K</sub> - <i>b</i> -PVP <sub>21.4K</sub>	61.02	28.85	7.35	2.73	22.35	10.57	8.30	3.93
PDMS <sub>10K</sub> - <i>b</i> -PVP <sub>13.9K</sub>	57.28	32.11	6.07	4.54	12.62	7.07	9.44	5.29
PDMS <sub>10K</sub> - <i>b</i> -PVP <sub>5.1K</sub>	47.43	39.22	3.55	9.76	4.86	4.02	13.36	11.04

**Figure 8.** X-ray diffraction patterns of PDMS<sub>10K</sub>-*b*-PVP<sub>21.4K</sub>, PDMS<sub>10K</sub>-*b*-PVP<sub>13.9K</sub> and PDMS<sub>10K</sub>-*b*-PVP<sub>5.1K</sub> copolymer fibers mats.**Figure 9.** Actin staining on 24 h fibroblasts interaction with three different PDMS-*b*-PVP fiber scaffolds: (A) Silicon wafer; (B) PDMS<sub>10K</sub>-*b*-PVP<sub>13.9K</sub>; (C) PDMS<sub>4.6K</sub>-*b*-PVP<sub>56.8K</sub>; (D) Bar 63x.

that PDMS<sub>4.6K</sub>-*b*-PVP<sub>56.8K</sub> is one good scaffold for fibroblast cells.

## 5. Conclusion

A novel fiber mats in the micro scale range and on the base of poorly studied copolymer poly(dimethylsiloxane-*b*-vinyl pyrrolidone) were successfully electrospun. During the electrospinning process, the fiber deposition onto the grounded collector was controlled by aluminum screen at different bend angles. The fiber morphology,

**Figure 10.** LDH test for cell proliferation of fibroblast on different PDMS-*b*-PVP scaffolds.

the thermal properties, surface chemical composition and crystalline structure of the novel materials were investigated in detail by numerous methods. It was found that these fibers possess strong hydrophilic properties evaluated by swelling properties and confirmed by water contact angle measurements. The presence of water in these block copolymer fibers changes strongly the  $T_g$  and  $T_m$  and fiber morphology as well. The biological response of the electrospun fiber mats was evaluated with human fibroblast cells.

We consider that this promising material, consisting of bioinert PDMS block and well known biocompatible and hydrophilic PVP block, possessing very interesting properties such as good biocompatibility and amphiphilicity reported here, and especially PDMS<sub>4.6K</sub>-*b*-PVP<sub>56.8K</sub> could find application as scaffold or nano carriers in tissue engineering and drug delivery systems.

## REFERENCES

- [1] S. Agarwal, J. H. Wendorff and A. Greiner, "Use of Electrospinning Technique for Biomedical Applications," *Polymer*, Vol. 49, No. 26, 2008, pp. 5603-5621. doi:10.1016/j.polymer.2008.09.014
- [2] T. J. Sill and H. A. von Recum, "Electrospinning: Applications in Drug Delivery and Tissue Engineering," *Biomaterials*, Vol. 29, No. 13, 2008, pp. 1989-2006. doi:10.1016/j.biomaterials.2008.01.011
- [3] D. H. Liang, B. S. Hsiao and B. Chu, "Functional Electrospun Nanofibrous Scaffolds for Biomedical Applica-

- tions," *Advanced Drug Delivery Reviews*, Vol. 59, No. 14, 2007, pp. 1392-1412. [doi:10.1016/j.addr.2007.04.021](https://doi.org/10.1016/j.addr.2007.04.021)
- [4] N. Ashammakhi, A. Ndreu, Y. Yang, H. Ylikauppila and L. Nikkola, "Applications in Drug Delivery and Tissue Engineering," *European Journal of Plastic Surgery*, Vol. 29, No. 13, 2008, pp. 238-333.
- [5] H. S. Yoo, T. G. Kim and T. G. Park, "Surface-Functionalized Electrospun Nanofibers for Tissue Engineering and Drug Delivery," *Advanced Drug Delivery Reviews*, Vol. 61, No. 12, 2009, pp. 1033-1042. [doi:10.1016/j.addr.2009.07.007](https://doi.org/10.1016/j.addr.2009.07.007)
- [6] M. Ma, R. M. Hill, J. L. Lowery, S. V. Fridrikh and Gregory C. Rutledge, "Electrospun Poly(Styrene-Block-Dimethylsiloxane) Block Copolymer Fibers Exhibiting Superhydrophobicity," *Langmuir*, Vol. 21, No. 12, 2005, pp. 5549-5554. [doi:10.1021/la047064y](https://doi.org/10.1021/la047064y)
- [7] S. Tungprapa, I. Jangchud, P. Ngamdee, M. Rutnakornpituk and P. Supaphol, "Surface-Functionalized Electrospun Nanofibers for Tissue Engineering and Drug Delivery," *Materials Letters*, Vol. 60, No. 12, 2006, pp. 2920-2924.
- [8] A. Alli, B. Hazer, Y. Menciloglu and S. Süzer, "Synthesis, Characterization and Surface Properties of Amphiphilic Polystyrene-b-Polypropylene Glycol Block Copolymers," *European Polymer Journal*, Vol. 42, No. 4, 2006, pp. 740-750. [doi:10.1016/j.eurpolymj.2005.09.032](https://doi.org/10.1016/j.eurpolymj.2005.09.032)
- [9] I. L. Keranov, F. di Lena, M. Michel, A. Kostadinova, V. Toniazzi, D. Ruch and T. Vladkova, "Synthesis, Characterization and Self-Assembling Properties of Amphiphilic Block Copolymers of Poly(n-Vinyl Pyrrolidone) and Poly(dimethylsiloxane)," *Journal of Applied Polymer Science*, Submitted for Revision.
- [10] G. Altankov, "Interaction of Cells with Biomaterial Surfaces," D.Sc. Thesis, Institute of Biophysics, BAS, Sofia, 2003.
- [11] N. Nyanik, B. Köker and Y. Yildiz, "Synthesis and Characterization of Poly(Dimethyl Siloxane) Containing Poly(Vinyl Pyrrolidinone) Block Copolymers," *Journal of Applied Polymer Science*, Vol. 71, No. 11, 1999, pp. 1915-1922. [doi:10.1002/\(SICI\)1097-4628\(19990314\)71:11<1915::AID-APP22>3.0.CO;2-D](https://doi.org/10.1002/(SICI)1097-4628(19990314)71:11<1915::AID-APP22>3.0.CO;2-D)